in the sympathetic nervous system. Decreased uptake of the tracers, 6F-DA or MIBG, was noted only in the heart, the thyroid gland and renal cortex, and the decrease in the heart was most prominent (5, 6, 29, 33). Moreover, there also seem to be differences among the parts of the heart. The PET study revealed that 6F-DA radioactivity was more severely decreased in the left ventricular free-wall than in the interventricular septum or the right myocardium (6, 12). Thus, the left ventricular anterior wall was expected to be one of the parts where the sympathetic nerve was most severely affected. We investigated this part of the heart pathologically and ascertained that the sympathetic nerves nearly disappeared.

There are several reports quantifying the TH protein content or TH activity in the central nervous system on postmortem examinations in PD. The TH protein content in PD decreased to 2.7% in the caudate nucleus, 5.3% in the putamen and 16% in substantia nigra compared with the control (17). TH activity decreased to 9.2% to 27.4% in the caudate nucleus, 4.1% to 21.6% in the putamen, 11.9% to 35.1% in the substantia nigra, 11.6% to 50.7% in the globus pallidus and 13% in the locus ceruleus (13, 16, 19). Our study revealed that in the epicardium of the left ventricular anterior wall, TH+ axons nearly completely disappeared in PD and the TH/fascicle ratio measured by quantitative analysis decreased to 1.1% of the control. Although there are differences in the measured object, it can be said that the cardiac sympathetic nerves in the left ventricular anterior wall are affected as much as the dopaminergic nerves in the central nervous system.

The sympathetic innervation to the ventricular working myocardium is thought to be mainly through the para-arterial route in the epicardium (15), consistent with the observation that the number of TH+ axons in the subepicardial area were larger than in the subendocardial area (11). The nerve fascicles in the epicardium, therefore, presumably contain sympathetic efferent axons innervating the working myocardium from the cervico/thoracic sympathetic ganglia. The depletion of TH+ axons in the epicardium represents the effacement of their distal axons and terminals, and therefore indicates cardiac sympathetic denervation in PD. The decreased cardiac uptake of these tracers is assumed to result from the effacement of these terminals since 6F-DA and MIBG are taken up by and stored in the adrenergic nerve terminals as with catecholamines (1, 38).

In addition, our study showed small number of myelinated axons in the epicardium, and the triple immunofluorolabeling unexpectedly demonstrated that some of the TH+ axons, although very small in number, were myelinated. The postganglionic sympathetic axons are generally considered unmyelinated C-fiber (35). Although the sympathetic afferent nerves consist of unmyelinated axons, it is uncertain and doubtful whether they are catecholaminergic. Neurotransmitters in the sympathetic afferent nerves are presumably considered substance P or neuropeptide K (26). As there was a report suggesting the existence of myelinated sympathetic postganglionic axons in a cat (3), our observation may indicate that the cardiac postganglionic sympathetic nerve contains tiny numbers of myelinated axons in humans.

In considering the pathogenesis of PD, the cardiac sympathetic nerves have not been emphasized as much as the central nervous system. This may be due to clinical absence of cardiac manifestations and the difficulty in detecting abnormalities. Because physiological functions of these sympathetic fibers in the myocardium are not well characterized, it is hard to predict the outcome after their depletion. Although diminished heart rate variability spectral measures of the variability have been reported in PD (8), routine electrocardiogram or ultrasound cardiography usually fail to demonstrate abnormalities. Indeed, all thirty-six PD patients in our previous study with decreased cardiac uptake of MIBG showed normal left ventricular function by ultrasound cardiography and most of them did not show serious arrhythmias and ST changes by 24-hour Holter electrocardiography (24). Among four PD patients in the present study, asymptomatic second degree A-V block of Mobitz type was the only abnormality in cardiac function. Because decreased cardiac uptake is not necessarily correlated with the presence of orthostatic hypotension nor with cardiac dysfunctions (5, 24), it is possible that near complete absence of sympathetic axons, first identified in the present study, is not related to clinically detectable manifestations. This is in agreement with the observation that left ventricular functions of transplanted heart under resting condition are quite normal even before sympathetic innervation is re-established (4). However, we should pay attention that decreased motor activity in PD patients may allow cardiac abnormalities, even if present, to remain unnoticed. Awareness of this sympathetic denervation, however, may raise attention to cardiac functions in PD patients and give clues to identify more subtle changes of cardiac functions so far not detectable but possibly linked to this sympathetic denervation.

This study demonstrated pathologically profound involvement in the cardiac sympathetic nervous system, which is catecholaminergic in common with the nigrostriatal nervous system. This may afford a new clue to elucidating the pathogenesis of PD.

REFERENCES

1. Chiueh CC, Zukowska-Grojec Z, Kirk KL, Kopin IJ (1983) 6-Fluorocatecholamines as false adrenergic neurotransmitters. *J Pharmacol Exp Ther* 225:529-533.

2. Chow LT, Chow WH, Lee JC, Chow SS, Anderson RH, Gosling JA (1998) Postmortem changes in the immunohistochemical demonstration of nerves in human ventricular myocardium. *J Anat* 192:73-80.

3. Emery DG, Foreman RD, Coggeshall RE (1978) Categories of axons in the inferior cardiac nerve of the cat. *J Comp Neurol* 177:301-310.

4. Frank MB, Peter U, Nina S, Stephan GN, Bruno R, Markus S (2001) Myocardial Efficacy and Sympathetic Reinnervation After Orthotopic Heart Transplantation. *Circulation* 103:1881-1886

5. Goldstein DS, Holmes CS, Dendi R, Bruce SR, Li ST (2002) Orthostatic hypotension from sympathetic denervation in Parkinson's disease. *Neurology* 58:1247-1255.

6. Goldstein DS, Holmes C, Li ST, Bruse S, Metman LV, Cannon RO (2000) Cardiac sympathetic denervation in Parkinson disease. *Ann Intern Med* 133:338-347.

7. Goto K, Longhurst PA, Cassis LA, Head RJ, Taylor DA, Rice PJ, Fleming WW (1985) Surgical sympathectomy of the heart in rodents and its effect on sensitivity to agonists. *J Pharmacol Exp Ther* 234:280-287.

8. Haapaniemi TH, Pursiainen V, Korpelainen JT, Huikuri HV, Sotaniemi KA, Myllyl VV (2001) Ambulatory ECG and analysis of heart rate variability in Parkinson's disease. *J Neurol Neurosurg Psychiatry* 70:305-310

9. Hardebo JE, Suzuki N, Ekblad E, Owman C (1992) Vasoactive intestinal polypeptide and acetylcholine coexist with neuropeptide Y, dopamine-beta-hydroxylase, tyrosine hydroxylase, substance P or calcitonin gene-related peptide in

neuronal subpopulations in cranial parasympathetic ganglia of rat. *Cell Tissue Res* 267:291-300.

10. Iwanaga K, Wakabayashi K, Yoshimoto M, Tomita I, Satoh H, Takashima H, Satoh A, Seto M, Tsujihata M, Takahashi H (1999) Lewy body-type degeneration in cardiac plexus in Parkinson's and incidental Lewy body diseases. *Neurology* 52:1269-1271.

11. Kawano H, Okada R, Yano K (2003) Histological study on the distribution of autonomic nerves in the human heart. *Heart Vessels* 18:32-39.

12. Li ST, Dendi R, Holmes C, Goldstein DS (2002) Progressive loss of cardiac sympathetic innervation in Parkinson's disease. *Ann Neurol* 52:220-223.

13. Lloyd KG, Davidson L, Hornykiewicz O (1975) The neurochemistry of Parkinson's disease: effect of L-dopa therapy. *J Pharmacol Exp Ther* 195:453-464.

14. Maccarrone C, Jarrott B (1987) Differential effects of surgical sympathectomy on rat heart concentrations of neuropeptide Y-immunoreactivity and noradrenaline. *J Auton Nerv Syst* 21:101-107.

15. Martins JB, Zipes DP (1980) Epicardial phenol interrupts refractory period responses to sympathetic but not vagal stimulation in canine left ventricular epicardium and endocardium. *Circ Res* 47:33-40.

16. McGeer PL, McGeer EG (1976) Enzymes associated with the metabolism of catecholamines, acetylcholine and gaba in human controls and patients with Parkinson's disease and Huntington's chorea. *J Neurochem* 26:65-76.

17. Mogi M, Harada M, Kiuchi K, Kojima K, Kondo T, Narabayashi H, Rausch D, Riederer P, Jellinger K, Nagatsu T (1988) Homospecific activity (activity per enzyme protein) of tyrosine hydroxylase increases in parkinsonian brain. *J Neural Transm* 72:77-82.

18. Molinoff PB, Axelrod J (1971) Biochemistry of catecholamines. *Annu Rev Biochem* 40:465-500.

19. Nagatsu T, Yamaguchi T, Rahman MK, Trocewicz J, Oka K, Hirata Y, Nagatsu I, Narabayashi H, Kondo T, Iizuka R (1984) Catecholamine-related enzymes and the biopterin cofactor in Parkinson's disease and related extrapyramidal diseases. *Adv Neurol* 40:467-473.

20. Nakamura A, Uchihara T (2004) Dual enhancement of triple immunofluorescence using two antibodies from the same species. *J Neurosci Methods* 135:67-70.

21. Neubauer B, Christensen NJ (1976) Norepinephrine, epinephrine, and dopamine contents of the cardiovascular system in long-term diabetics. *Diabetes* 25:6-10.

22. Orimo S, Oka T, Miura H, Tsuchiya K, Mori F, Wakabayashi K, Nagao T, Yokochi M (2002) Sympathetic cardiac denervation in Parkinson's disease and pure autonomic failure but not in multiple system atrophy. *J Neurol Neurosurg Psychiatry* 73:776-777.

23. Orimo S, Ozawa E, Nakade S, Hattori H, Tsuchiya K, Taki K, Takahashi A (2003) [^{123}I] metaiodobenzylguanidine myocardial scintigraphy differentiates corticobasal degeneration from Parkinson's disease. *Intern Med* 42:127-128.

24. Orimo S, Ozawa E, Nakade S, Sugimoto T, Mizusawa H (1999) ^{123}I-metaiodobenzylguanidine myocardial scintigraphy in Parkinson's disease. *J Neurol Neurosurg Psychiatry* 67:189-194.

25. Orimo S, Ozawa E, Oka T,Nakade S, Tsuchiya K, Yoshimoto M, Wakabayashi K, Takahashi H (2001) Different histopathology accounting for a decrease in myocardial MIBG uptake in PD and MSA. *Neurology* 57:1140-1141.

26. Owman C (1988) Autonomic innervation of the cardiovascular system. In: *Handbook of Chemical Neuroanatomy*, Bjorklund A, Hokfelt T (eds.), Volume 6, The Peripheral Nervous System, Chapter IX, pp.327-340, Elsevier: Amsterdam, New York, Oxford

27. Pardini BJ, Lund DD, Schmid PG (1990) Innervation patterns of the middle cervical--stellate ganglion complex in the rat. *Neurosci Lett* 117:300-306.

28. Petch MC, Nayler WG (1979) Concentration of catecholamines in human cardiac muscle. *Br Heart J* 41:340-344

29. Reinhardt MJ, Jungling FD, Krause TM, Braune S (2000) Scintigraphic differentiation between two forms of primary dysautonomia early after onset of autonomic dysfunction: value of cardiac and pulmonary iodine-123 MIBG uptake. *Eur J Nucl Med* 27:595-600.

30. Schuurman HJ, Plomp S, Wijngaard PL, Slootweg PJ, de Jonge N (1993) Innervation of the endomyocardium in the first period after heart transplantation. *Transplantation* 56:85-88.

31. Singh S, Johnson PI, Javed A, Gray TS, Lonchyna VA, Wurster RD (1999) Monoamine- and histamine-synthesizing enzymes and neurotransmitters within neurons of adult human cardiac ganglia. *Circulation* 99:411-419.

32. Takahashi A (1991) Autonomic nervous system disorders in Parkinson's disease. *Eur Neurol* 31(Suppl 1):41-47.

33. Taki J, Nakajima K, Hwang EH, Matsunari I, Komai K, Yoshita M, Sakajiri K, Tonami N (2000) Peripheral sympathetic dysfunction in patients with Parkinson's disease without autonomic failure is heart selective and disease specific. *Eur J Nucl Med* 27:566-573.

34. Uchihara T, Nakamura A, Nakayama H, Arima K, Ishizuka N, Mori H, Mizushima S (2003) Triple immunofluorolabeling with two rabbit polyclonal antibodies and a mouse monoclonal antibody allowing three-dimensional analysis of cotton wool plaques in Alzheimer disease. *J Histochem Cytochem* 51:1201-1206.

35. Van Stee EW (1978) Autonomic innervation of the heart. *Environ Health Perspect* 26:151-158.

36. Wakabayashi K, Takahashi H (1997) Neuropathology of autonomic nervous system in Parkinson's disease. *Eur Neurol* 38 Suppl 2:2-7.

37. Wharton J, Polak JM, Gordon L, Banner NR, Springall DR, Rose M, Khagani A, Wallwork J, Yacoub MH (1990) Immunohistochemical demonstration of human cardiac innervation before and after transplantation. *Circ Res* 66:900-912.

38. Wieland DM, Brown LE, Tobes MC, Rogers WL, Marsh DD, Mangner TJ, Swanson DP, Beierwaltes WH (1981) Imaging the primate adrenal medulla with [^{123}I] and [^{131}I] meta-iodobenzylguanidine: concise communication. *J Nucl Med* 22:358-364.

39. Yoshita M (1998) Differentiation of idiopathic Parkinson's disease from striatonigral degeneration and progressive supranuclear palsy using iodine-123-meta iodobenzylguanidine myocardial scintigraphy. *J Neurol Sci* 155:60-67.

Acta Neuropathol (2005) 109: 159–164
DOI 10.1007/s00401-004-0922-3

REGULAR PAPER

Toshiki Uchihara · Charles Duyckaerts
Danielle Seilhean · Ayako Nakamura
Françoise Lazarini · Jean-Jacques Hauw

Exclusive induction of tau2 epitope in microglia/macrophages in inflammatory lesions—tautwopathy distinct from degenerative tauopathies

Received: 13 May 2004 / Revised: 2 August 2004 / Accepted: 2 August 2004 / Published online: 12 November 2004

Abstract Tau2 antibody recognizes a phosphorylation-independent epitope that is pathologically modified as tau protein is phosphorylated to form neurofibrillary tangles of Alzheimer's disease (AD). Similar modification of tau2 epitope can be induced even in the absence phosphorylation of tau, as we first demonstrated in ischemic foci and in glial cytoplasmic inclusions (GCIs) of multiple system atrophy. This modification of tau2 epitope is distinguishable from those observed in degenerative tauopathies because (1) it is a conformational change, which is reversible upon exposure to a detergent; (2) it shows an absence of fibrils composed of phosphorylated tau protein; and (3) it is characterized by the lack of immunohistochemical labeling by anti-tau antibodies other than tau2. In this study, we expanded this observation to inflammatory foci of different pathologies (human immunodeficiency virus encephalopathy, progressive multifocal leukoencephalopathy or multiple sclerosis) by examining formalin-fixed, paraffin-embedded sections immunostained with a panel of anti-tau antibodies. It was found that tau2 was the only anti-tau antibody that immunolabeled microglia/macrophages in these lesions, and this immunoreactivity was reversibly diminished upon exposure to a detergent. Exclusive apparition of tau2 immunoreactivity in these cells without neurofibrillary pathology may be a secondary event shared with ischemic foci and GCIs. It is, however, related to a unique conformational state of tau, possibly grouped under the name of "tautwopathy", that may represent an initial stage of tau deposition distinct from degenerative tauopathies characterized by fibrils composed of phosphorylated tau protein.

Keywords Tauopathy · Tautwopathy · Multiple sclerosis · Progressive multifocal leukoencephalopathy · HIV encephalopathy

T. Uchihara (✉) · A. Nakamura
Department of Neuropathology,
Tokyo Metropolitan Institute for Neuroscience,
2-6 Musashi-dai, Fuchu, 183-8526 Tokyo, Japan
E-mail: uchihara@tmin.ac.jp
Tel.: +81-42-3253881
Fax: +81-42-3218678

T. Uchihara · C. Duyckaerts · D. Seilhean · F. Lazarini
J.-J. Hauw
Laboratoire Raymond Escourolle, Service de Neuropathologie,
Hôpital de la Salpêtrière, Association Claude Bernard,
Université Paris VI, 47 Boulevard de l'Hôpital,
75651 Paris Cedex 13, France

Introduction

Tau deposition is one of the major neuropathological hallmarks for a variety of neurodegenerative disorders, grouped under the name of tauopathy. In our previous immunohistochemical studies on human brains with cerebral infarction, obtained at autopsy, we reported the presence of Alz-50 [22] and tau2 immunoreactivity (IR) [24] in neurons and microglia/macrophages, respectively, and demonstrated that tau deposition was not a specific phenomenon restricted to degenerative tauopathies. Subsequent studies on human brains demonstrated that tau protein in ischemic foci was not phosphorylated, and the tau2 IR was reversibly abolished upon exposure to a detergent [28]. Interestingly, similar changes were observed for glial cytoplasmic inclusions (GCIs) of multiple system atrophy (MSA) [21]. The absence of neurofibrillary changes in these tau2-immunopositive cells in ischemic foci and GCIs indicates that tau deposition, by itself, does not necessarily lead to neurofibrillary changes in human brains. Because modification of tau protein is a prerequisite for immunohistochemical visualization on formalin-fixed, paraffin-embedded sections [12, 18], identification of specific changes in these non-fibrillary tau deposits will potentially clarify differences among a variety of tau deposits. In the present

study, we expanded this observation by examining tau-immunostained sections in the vicinity of inflammatory foci of different pathologies. This is the first study demonstrating that induction of tau2 IR in activated microglia/macrophages, which is distinct from neurofibrillary changes, is a phenomenon shared by a variety of inflammatory processes as well as by ischemia and GCIs of MSA.

Materials and methods

Five cases with human immunodeficiency virus (HIV) encephalopathy (age at death: 23–42 years), four cases with progressive multifocal leukoencephalopathy (PML) (age at death: 35–85 years) and six cases with multiple sclerosis (MS) (age at death: 30–57 years) were enrolled in this study. Formalin-fixed, paraffin-embedded blocks containing active foci with glial reactions were obtained. Deparaffinized sections were treated with 1% H_2O_2 for 20 min followed by blocking with 5% normal serum. The sections were immunostained with one of the anti-tau antibodies (tau2 [16, 17], 1:1,000, Sigma, Saint Louis, MO; AT8 [13], 1:10,000, Innogenetics, Zwinjndrecht, Belgium; anti-human tau (pool 2) [5], 1:10,000, a generous gift from Prof. H. Mori, Osaka City University; tau-1 [17], 1:10,000, Boehringer, Manheim, Germany; or Alz-50, 1:200, a generous gift from Prof. P. Davies [30]) using the avidin-biotin-peroxidase complex (ABC) method with diaminobenzidine and nickel ammonium sulfate as chromogen, which yielded a deep purple reaction product. Specificity of tau2 IR was established previously both on immunoblot and histological sections from human brains [21, 28]. Preabsorption of tau2 antibody with a synthetic peptide corresponding to the tau2 epitope (AGIGDTSNLEDQAA [29] 1 μg/ml) or with the same concentration (1 μg/ml) of Fc fragment of human IgG (Athens Research & Technol Inc, Athens, GA) was performed in parallel. Omission of the primary antibody served as negative control to see whether secondary antibodies (biotinylated anti-mouse IgG or biotinylated anti-human IgG, Vector) yielded nonspecific labeling mediated, for example, through Fc receptors possibly present on microglial cells. The influence of detergent on tau2 IR was examined, as reported previously on human brains with infarction, AD [28], Down's syndrome and MSA [21], by incubating the sections with tau2 antibody diluted in phosphate-buffered saline (PBS) with or without 0.03% polyoxylethyleneglycol-*p*-isooctylphenyl ether (Triton X-100, TX). In parallel, preincubation with PBS containing 0.03% TX was followed by washing with PBS not containing TX before tau2 immunostaining.

When necessary, the tau2-immunostained sections were subsequently subjected to the second cycle immunostaining with either anti-ferritin (rabbit polyclonal, 1:1,000, DAKO, Glostrup, Denmark) or anti-glial fibrillary acidic protein (GFAP; rabbit polyclonal, 1:10,000, DAKO) antibody. Omission of nickel ammonium sulfate from the chromogen yielded a brown reaction product for these second-cycle antibodies. Double immunostaining with two different monoclonal antibodies (anti-gp24 against HIV, DAKO and tau2) was performed as follows [9, 15, 27]. Tau2 antibody was diluted 1:10,000, and was probed by an anti-mouse IgG conjugated with horseradish peroxidase (HRP; 1:1,000, Kirkegaard Perry, Gaithersburg, MD). The HRP signal was amplified using biotinylated tyramide (1:1,000) in the presence of 0.01% H_2O_2 [1]. After incubation with streptavidin-conjugated HRP (1:200, Vector, Burlingame, CA), color development was performed with diaminobenzidine and nickel ammonium sulfate to yield a deep purple reaction product. These tau2-immunostained sections were then subjected to the second-cycle immunostaining with another mouse monoclonal antibody against gp24 using the ABC method. The amplification performed with biotinylated tyramide in the first cycle was so sensitive that the primary antibody tau2 could be diluted to 1:10,000; however, the ABC method used in the second cycle was not sensitive enough to detect this dilution (1:10,000) of tau2 antibody, and exclusively visualized the gp24 epitope. Omission of nickel ammonium sulfate from the chromogen yielded a brown reaction product for the gp24 epitope.

Results

Microglia/macrophages, major components in these inflammatory processes of these brains, contained tau2 IR in all the sections examined, regardless of the diagnosis (Fig. 1A PML, D MS, G HIV encephalopathy). Tau2 IR in these cells was abolished when the primary antibody was diluted in PBS containing 0.03%TX (Fig. 1B, E, H). Disappearance of tau2 IR upon exposure to TX was reversed when the sections, preincubated with 0.03%TX, were washed with PBS not containing TX before immunostaining (Fig. 1C, F, J). This tau2 IR (Fig. 2A, at the periphery of a demyelinating focus of MS) was abolished when the antibody was co-incubated with the synthetic peptide corresponding to its target epitope [29] (Fig. 2B, the same area as Fig. 2A). Co-incubation of the Fc fragment of human IgG with tau2 failed to eliminate this tau2 IR (data not shown). Preincubation of the section with an excess amount (10 μg/ml) of the Fc fragment also failed to eliminate tau2 IR (data not shown). Finally, direct probing of the section either with biotinylated anti-mouse IgG or biotinylated anti-human IgG, followed by ABC method, visualized no IR (data not shown). These data indicate that immunoreaction with tau2 is specific for the tau2 epitope and is not due to nonspecific reactions, for example, mediated by the Fc receptor potentially expressed on the surface of microglial cells. These tau2-immunoreactive cells were not co-labeled with anti-GFAP (Fig. 2C, a lesion of PML), and double labeling

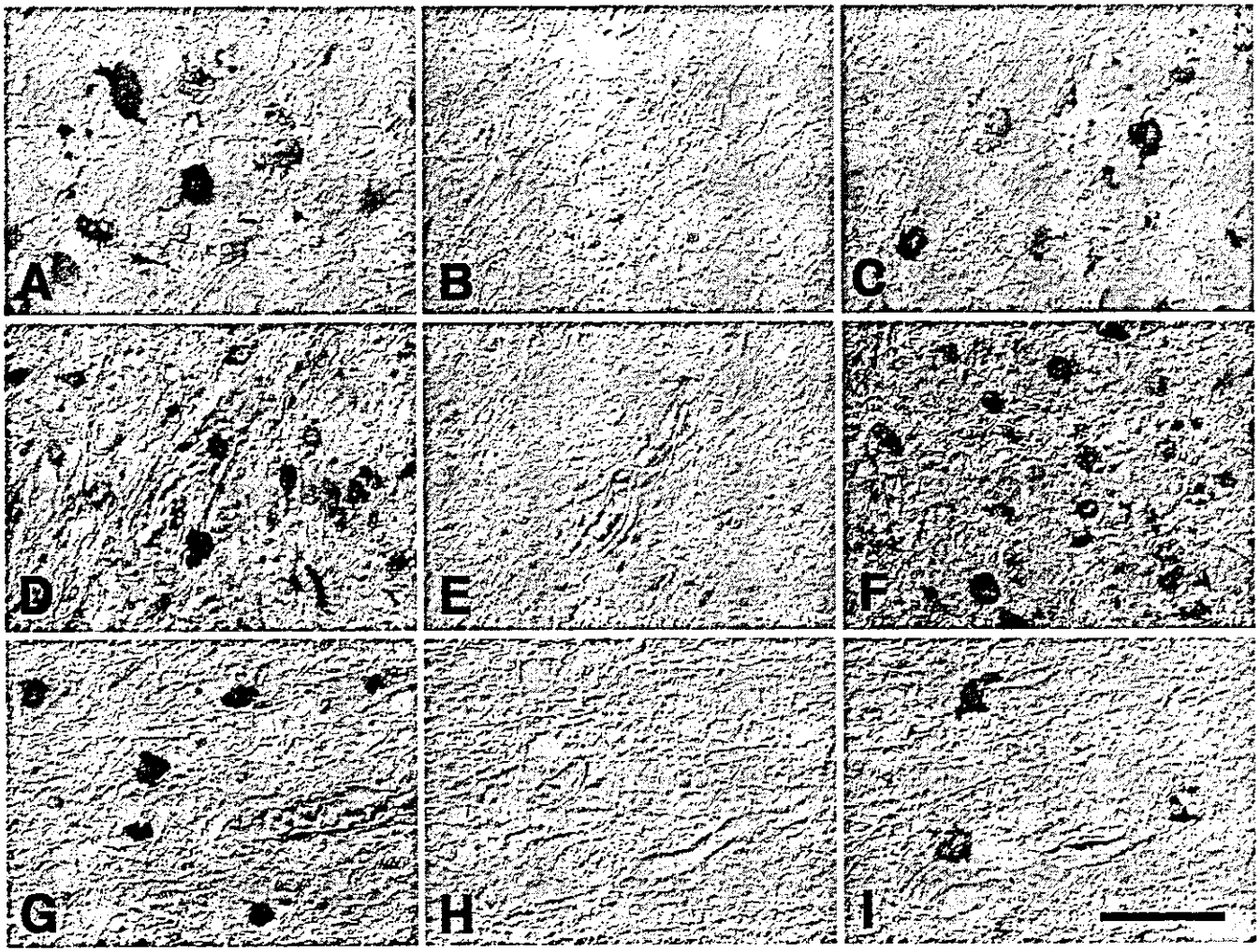

Fig. 1 Tau2-immunoreactive cells in PML (A–C), MS (D–F) and HIV encephalopathy (G–I). Tau2 IR (A PML, D MS, G HIV) is abolished when the primary antibody is diluted in buffer containing 0.03% TX (B PML, E MS, H HIV). This abolished tau2 IR upon exposure to TX (B, E, H) is restored after washing (C, F, I) [*PML* progressive multifocal leukoencephalopathy, *MS* multiple sclerosis, *HIV* human immunodeficiency virus, *IR* immunoreactivity, *TX* Triton X-100 (polyoxylethyleneglycol-*p*-isooctylphenyl ether)]. *Bar* 50 μm

immunohistochemistry with tau2 and anti-ferritin antibody demonstrated the colocalization of these two epitopes (Fig. 2D, HIV encephalopathy), confirming the microglial origin of these tau2-immunopositive cells. In brains with HIV encephalopathy, perivascular aggregates of microglia/macrophages (Fig. 2D) and giant multinucleated cells (Fig. 2E, arrow) contained tau2 IR. Double labeling with tau2 (deep purple) and anti-gp24 (brown) demonstrated that these epitopes were colocalized to microglia/macrophages (Fig. 2E). Modified oligodendrocytes found in PML brains did not exhibit tau2 IR (Fig. 2F, arrow). The panel of anti-tau antibodies other than tau2 failed to immunostain these microglia/macrophages. Neurofibrillary changes were absent on sections stained with the Gallyas silver impregnation method.

Discussion

In previous immunohistochemical studies on human brains with cerebral infarction, we reported that tau epitopes were induced differently in neurons and glial cells after an ischemic insult, where microglia/macrophages exhibited tau2 IR [24], while neurons contained Alz-50-positive granules in the cytoplasm [22]. In a subsequent study, we demonstrated that the modification of tau, linked to its immunohistochemical visualization around ischemic foci, was not necessarily related to its pathological phosphorylation [28]. In the present study, we wanted to expand this observation by examining sections from inflammatory processes of different etiologies to see whether tau2 IR is also induced in microglia/macrophages. Among the panel of anti-tau antibodies, tau2 was the only antibody that visualized the tau epitope in these inflammatory processes. The presence of the tau2 epitope exclusively in microglia/macrophages lacking neurofibrillary changes indicates that the modification of tau2 epitope in these inflammatory processes is similar to that reported for cerebral infarction [24, 28] and GCIs of MSA [21]. It is, therefore, not plausible that visualization of tau2 epitope represents an excessive

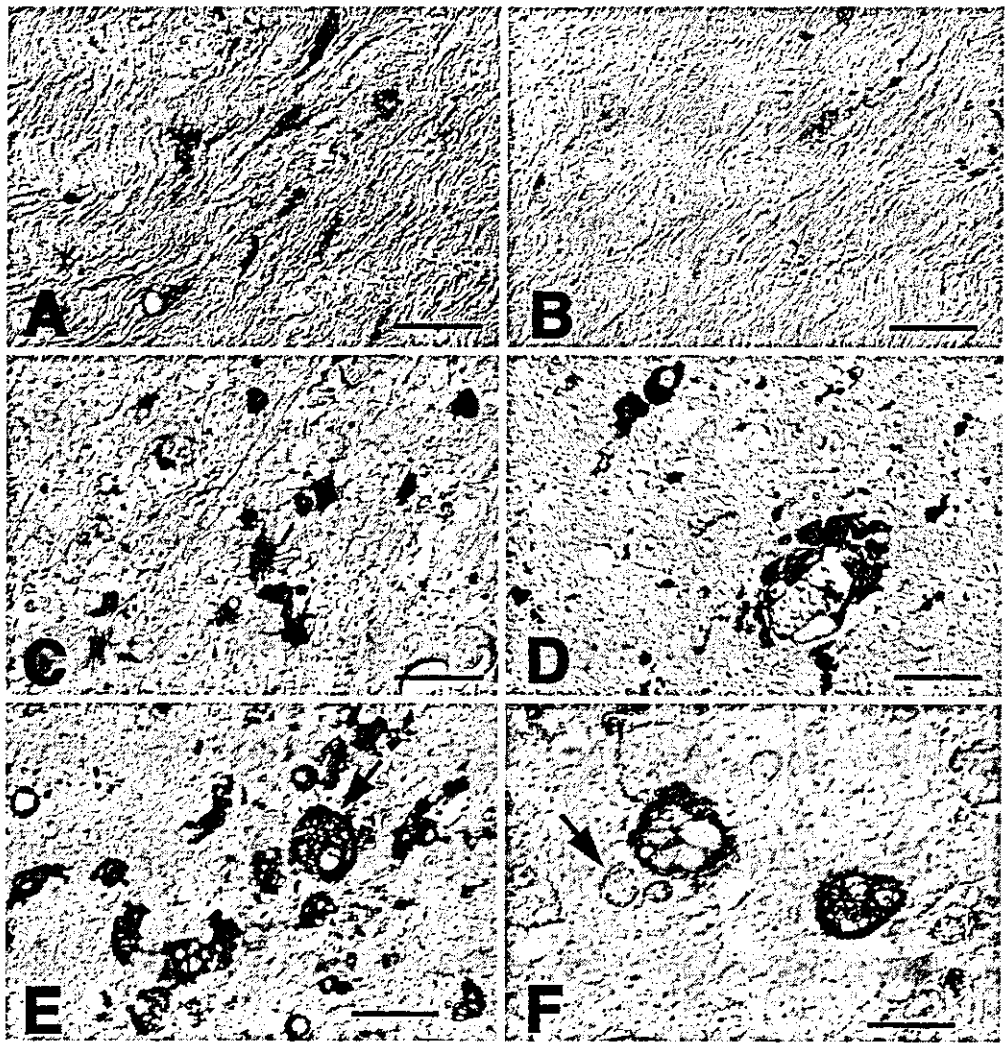

Fig. 2 A Tau2-immunoreactive glial cells at the periphery of a demyelinating focus (MS) in the internal capsule. B Co-incubation of tau2 with a synthetic peptide mimicking tau2 epitope abolishes the IR (the same area of the same case as A). C Double immunostaining with tau2 (*purple*) and an anti-GFAP antibody (*brown*) in a lesion of PML. Tau2 and GFAP epitopes are expressed in different cells without overlap. D Double immunostaining with tau2 (*purple*) and an anti-ferritin antibody (*brown*) in the white matter of the brain with HIV encephalopathy. Perivascular cells are immunopositive for both tau2 and ferritin, indicating that perivascular microglia/macrophages exhibit tau2 IR. E Double immunostaining with tau2 (*violet*) and gp24 (*brown*) in the white matter of the brain with HIV encephalopathy. Glial cells immunopositive for gp24, including multinucleated giant cells (*arrow*), exhibit tau2 IR. F Tau2 immunostain (*brown*) counterstained lightly with hematoxylin in the white matter of the brain with PML. Numerous phagosomes of macrophages are surrounded by tau2 IR, while this IR is not detectable in modified oligodendrocytes (*arrow*) (*GFAP* glial fibrillary acidic protein). *Bars* A–E 50 μm, F 25 μm

accumulation of tau. It rather indicates that modification of the tau epitope is too limited to involve the entire extent of the tau protein. Moreover, tau2 IR was restricted to the cytoplasm without extracellular deposits, which suggests its endogenous origin. Several tau epitopes, including tau2, are usually detectable on immunoblots of normal brain extract. Their immunohistochemical visualization is, however, usually difficult on sections from normal brains fixed with formalin. Tau2 antibody, however, immunolabels neurofibrillary tangles (NFTs) even after fixation with formalin [16, 17]. This discrepancy between immunoblot and immunohistochemistry is explainable if these tau epitopes in brain tissue remain active after fixation only when tau molecules are modified into a pathological state [8, 12, 18, 22, 28]. Immunohistochemical visualization of tau2 epitope is dependent on proline[101] of human tau, which was reported to be transformed into a serine-like conformation when tau protein is integrated into paired helical filaments of AD after pathological phosphorylation [11, 16, 17, 29]. One might, then, suppose that some pathological events involving tau2 epitope, not necessarily linked to phosphorylation, are responsible for its immunohistochemical visualization on formalin-fixed tissue. Indeed, this was proved to be the case in our previous studies on ischemia [28] and GCIs [21].

In contrast to neurofibrillary changes seen in AD brains, the Alz-50 IR in the cytoplasm of neurons around

the ischemic focus is granular, without fibrillary structure or argyrophilia [4, 22], as observed in pretangle neurons of the hippocampus of AD brains [3]. Tau2-immunoreactive microglia/macrophages seen in inflammatory or ischemic foci also failed to exhibit argyrophilic fibrillary features, suggesting that possible conformational changes of the tau molecule involved in these conditions are different from those of AD. Moreover, exposure to TX abolished tau2 IR in these microglia/macrophages, as observed around ischemic foci [28] and GCIs [21]. Because tau2 IR on NFTs of AD are more resistant to TX exposure [28], relative sensitivity of tau2 IR to TX shared among microglia/macrophages in ischemic foci, inflammatory processes and in GCIs is another characteristic feature of these tau2 deposits. Tau2 deposition is not a primary event in these processes. Modification of tau, with special reference to tau2 epitope, as we demonstrated in ischemia, inflammation and GCIs, is distinguishable from so-called "degenerative tauopathies". This distinction is based on a conformational change of the tau2 epitope that is reversible upon exposure to a detergent, the absence of fibrils composed of phosphorylated tau protein, and is characterized by the lack of immunohistochemical labeling by anti-tau antibodies other than tau2. We therefore propose the term "tautwopathy", to draw attention to these characteristics that are distinct from "degenerative tauopathies". If one is not aware of this distinction, immunohistochemical visualization of tau2 epitope could be confounded with degenerative tauopathy [6, 10].

We do not yet know, however, the underlying mechanisms that potentially differentiate these two distinct types of tau deposition. One possibility is that tautwopathy represents an early phase of tau deposition before fibril formation. The lack of fibrillary structure is compatible with the relative sensitivity to TX. If tautwopathy was a prelude to "degenerative tauopathy", tau deposition might precede phosphorylation. Another interpretation is that modification of tau2 epitope could be totally independent of tau phosphorylation seen in degenerative tauopathies. Preferential involvement of glial cell in tautwopathy supports this hypothesis. These two interpretations are, however, not mutually exclusive and tautwopathic processes may occur during degenerative tauopathies. Even if tau expression is a ubiquitous phenomenon irrespective of the cell type, there are still differences in tau epitopes visualized, and in the conformational states, that depend on the cell type and the disease process [23, 25, 26]. In addition, we do not know how these differences in tau deposition are brought about. Modification of or difference in the tau molecule itself (for example phosphorylation or truncation) [20], its association of other molecules [2, 7, 14, 19] or other environmental factors are possible candidates to explain these differences. Although tautwopathy is a secondary phenomenon, awareness of it will improve the understanding of the deposition of any kind tau, by providing another reference distinct from degenerative tauopathies.

Acknowledgements The authors thank Professors H. Mori (Osaka City University) and P. Davies for providing the anti-tau antibodies. This work was supported in part by the grants from the Ministry of Education, Culture, Sports, Science and Technology (grant in aid for scientific research B1530118) and from Ministry of Health, Welfare and Labor (Longevity Science H-14-005).

References

1. Adams JC (1992) Biotin amplification of biotin and horseradish peroxidase signals in histochemical stains. J Histochem Cytochem 40:1457–1463
2. Arrasate M, Peres M, Valpuesta JM, Aliva J (1997) Role of glycosaminoglycans in determining the helicity of paired helical filaments. Am J Pathol 151:1115–1122
3. Bancher C, Brunner C, Lassman H, Budka H, Jellinger K, Wiche G, Seiterberger F, Grundke-Iqbal I, Wisniewski HM (1989) Accumulation of abnormally phosphorylated tau precedes the formation of neurofibrillary tangles in Alzheimer's disease. Brain Res 477:90–99
4. Dewar D, Graham DI, Teasdale GM, McCulloch J (1993) Alz-50 and ubiquitin immunoreactivity is induced by permanent focal cerebral ischemia in the cat. Acta Neuropathol 86:623–629
5. Endoh R, Ogawara M, Iwatsubo T, Nakano I, Mori H (1993) Lack of carboxy terminal sequence of tau in ghost tangles of Alzheimer's disease. Brain Res 601:164–172
6. Forno LS, Langston JW, Herrick MK, Wilson JD, Murayama S (2002) Ubiquitin-positive neuronal and tau2-positive glial inclusions in frontotemporal dementia of motor neuron type. Acta Neuropathol 130:599–606
7. Goedert M, Jakes R, Spillantini MG, Hasegawa M, Smith MJ, Crowther RA (1996) Assembly of microtubule-associated protein tau into Alzheimer-like filaments induced by sulphated glycosaminoglycans. Nature 383:550–553
8. Grundke-Iqbal I, Iqbal K, Tung YC, Quinlan M, Wisniewski HM, Binder LI (1986) Abnormal phosphorylation of the microtubule-associated protein tau (tau) in Alzheimer cytoskeletal pathology. Proc Natl Acad Sci USA 83:4913–4917
9. Hunyaday B, Krempels K, Harta G, Mezey E (1996) Immunohistochemical signal amplification by catalyzed reporter deposition and its amplification in double immunostaining. J Histochem Cytochem 44:1353–1362
10. Kertesz A, Kawarai T, Rogaeva E, St. George-Hyslop P, Poorkaj P, Bird TD (2000) Familial frontotemporal dementia with ubiquitin-positive, tau-negative inclusions. Neurology 54:818–827
11. Lang E, Otvos L (1992) A serine → proline change in Alzheimer's disease-associated epitope tau2 results in altered secondary structure, but phosphorylation overcomes the conformational gap. Biochem Biophys Res Commun 188:162–169
12. Matsuo ES, Shin R-W, Billingsley ML, Van deVoorde A, O'Connor M, Trojanowski JQ, Lee VM-Y (1994) Biopsy-derived adult human brain tau is phosphorylated at many of the same sites as Alzheimer's disease paired helical filament tau. Neuron 13:989–1002
13. Mercken M, Vandermeern M, Lübke U, Six J, Boons J, Van de Voorde A, Martin J-J, Gheuens J (1992) Monoclonal antibodies with selective specificity for Alzheimer tou are directed against phosphatase-sensitive epitopes. Acta Neuropathol 84:265–272
14. Murayama H, Shin R-W, Higuchi J, Shibuya S, Muramoto T, Kitamoto T (1999) Interaction of alminium with PHF tau in Alzheimer's disease neurofibrillary degeneration evidenced by desferrioxamine-assisted chelating autoclave method. Am J Pathol 155:877–885
15. Nakamura A, Uchihara T (2004) Dual enhancement of triple immunofluorescence using two antibodies from the same species. J Neurosci Methods 135:67–70

16. Papasozomenos SC (1989) Tau protein immunoreactivity in dementia of the Alzheimer type. I. Morphology, evolution, distribution, and pathogenetic implications. Lab Invest 60:123–137
17. Papasozomenos SC, Binder LI (1987) Phosphorylation determines two distinct species of tau in the central nervous system. Cell Motil Cytoskel 8:210-226
18. Pollock NJ, Wood JG (1988) Differential sensitivity of the microtubule associated protein, tau, in Alzheimer's disease tissue to formalin fixation. J Histochem Cytochem 36:1117–1121
19. Sayre LM, Perry G, Harris PLR, Liu Y, Schubert KA, Smith MA (2000) In situ oxidative catalysis by neurofibrillary tangles and senile plaques in Alzheimer's disease: a central role for bound transition metal. J Neurochem 74:270–279
20. Sergeant N, Wattez A, Delacourte A (1999) Neurofibrillary degeneration in progressive supranuclear palsy and corticobasal degeneration: tau pathologies with exclusively "exon 10" isoforms. J Neurochem 72:1243–1249
21. Shibuya K, Uchihara T, Nakamura A, Ishiyama M, Yamaoka K, Yagishita S, Iwabuchi K, Kosaka K (2003) Reversible conformational change of tau-2 epitope exposed to detergent in glial cytoplasmic includions in multiple system atrophy. Acta Neuropathol 105:508–514
22. Uchihara T, Tsuchiya K, Kondo H, Hayama T, Ikeda K (1995) Widespread appearance of Alz-50 immunoreactive neurons in the human brain with cerebral infarction. Stroke 26:2145–2148
23. Uchihara T, Nakamura A, Yamazaki M, Mori O (2000) Tau-positive neurons in corticobasal degeneration and Alzheimer's disease—distinction by thiazin red and silver impregnations. Acta Neuropathol 100:385–389
24. Uchihara T, Tsuchiya K, Nakamura A, Ikeda K (2000) Appearance of tau-2 immunoreactivity in glial cells in human brain with cerebral infarction. Neurosci Lett 286:99–102
25. Uchihara T, Nakamura A, Yamazaki M, Mori O (2001) Evolution from pretangle neurons to neurofibrillary tangles monitored by thiazin red combined with Gallyas method and double immunofluorescence. Acta Neuropathol 101:535–539
26. Uchihara T, Nakamura A, Yamazaki M, Mori O, Ikeda K, Tsuchiya K (2001) Different conformation of neuronal tau deposits distinguished by double immunofluorescence with AT8 and thiazin red combined with Gallyas method. Acta Neuropathol 102:462–466
27. Uchihara T, Nakamura A, Nakayama H, Arima K, Ishizuka N, Mori H, Mizushima S (2003) Triple immunofluorolabeling with two rabbit polyclonal antibodies and a mouse monoclonal antibody allowing three-dimensional analysis of cotton wool plaques in Alzheimer disease. J Histochem Cytochem 51:1201–1206
28. Uchihara T, Nakamura A, Arai T, Ikeda K, Tsuchiya K (2004) Microglial tau undergoes phosphorylation-independent modification after ischemia. Glia 45:180–187
29. Watanabe N, Takio K, Hasegawa M, Arai T, Titani K, Ihara Y (1992) Tau 2: a probe for a Ser conformation in the amino terminus of tau. J Neurochem 58:960–966
30. Wolozin BL, Pruchnicki A, Dickson DW, Davies P (1986) A neuronal antigen in the brains of Alzheimer's patients. Science 232:648–650

Acta Neuropathologica

10.1007/s00401-004-0947-7

Regular Paper

Silver stains distinguish tau-positive structures in corticobasal degeneration/progressive supranuclear palsy and in Alzheimer's disease—Comparison between Gallyas and Campbell-Switzer methods

Toshiki Uchihara[1] ✉, **Katsuhiko Shibuya**[1, 2], **Ayako Nakamura**[1] **and Saburo Yagishita**[3]

(1) Department of Neuropathology, Tokyo Metropolitan Institute for Neuroscience, 2-6 Musashi-dai, Fuchu, 183-8526 Tokyo, Japan

(2) Department of Neurology and Psychiatry, Kanagawa Rehabilitation Center, Kanagawa, Japan

(3) Department of Pathology, Kanagawa Rehabilitation Center, Kanagawa, Japan

✉ **Toshiki Uchihara**
Email: uchihara@tmin.ac.jp
Phone: +81-42-3253881 ext 4712
Fax: +81-42-3218678

Received: 3 September 2004 **Revised:** 15 October 2004 **Accepted:** 18 October 2004 **Published online:** 24 December 2004

Abstract Possible differences in silver-staining profiles and their relation to tau-like immunoreactivity were investigated on cortical sections from corticobasal degeneration (CBD), progressive supranuclear palsy (PSP), Down's syndrome (DS) and Alzheimer's disease (AD). Pairs of mirror sections were double-fluorolabeled with an anti-PHF tau (AT8) antibody and thiazin red (TR), a fluorochrome that labels fibrillary structures such as neurofibrillary tangles (NFTs). Subsequently, one of the pair was stained with Gallyas method (GAL), and the other with Campbell-Switzer method (CS). Identification of the same structure on the corresponding microscopic fields enabled a comparison of four different profiles of each structure: AT8 immunoreactivity, and affinity to TR, GAL and CS. NFTs of DS/AD, containing three- and four-repeat tau, were positive for TR, GAL and CS. AT8-immunoreactive structures of CBD/PSP, containing mainly four-repeat tau, were positive for GAL, but negative for CS and TR. This discrepancy is explainable if the argyrophilia with GAL is related to deposits containing four-repeat tau, while that with CS is linked to those containing three-repeat tau. The lack of CS labeling may also be related to poor TR staining, possibly representing scarcity of fibrillary structure in CBD/PSP. The absence of CS staining is characteristic of tau-positive structures of CBD/PSP, which is readily distinguishable from NFTs of DS/AD, hence is of potential pathological and diagnostic relevance.

Keywords Argyrophilia - Campbell-Switzer - Diagnosis - Gallyas - Three/four-repeat tau

Introduction

Deposition of tau is a hallmark for degenerative tauopathies, currently classified according to the difference in molecular species (three-repeat or four-repeat) of pathologically phosphorylated tau [*26*]. In spite of this biochemical difference, it is still difficult to differentiate them based on the immunostaining profiles of tau-positive deposits [*5*, *6*, *10*, *21*, *37*]. Another way to identify these deposits in tauopathies is silver staining. Early observations on neurofibrillary tangles (NFTs) and senile plaques (SPs) were based on silver-staining methods. They have been used for diagnosis of these tauopathies and Alzheimer's disease (AD), and are still being improved [*1*, *2*, *7*, *9*, *13*, *16*, *17*, *23*, *35*]. Further improvements of silver-staining methods [*3*, *4*, *19*, *27*] have been claimed based on enhanced sensitivity with less background and easier standardization of the procedure. The Gallyas method (GAL) [*13*] and its modification [*4*] is one of the successful examples in clearly visualizing tau- or synuclein-containing deposits. Up to now, various silver-staining methods have been compared for their sensitivity in detecting AD-related deposits [*8*, *12*, *20*, *24*, *32*, *33*, *34*, *36*]. Among them, GAL was found to be very sensitive in detecting NFTs of AD [*20*, *24*, *33*]. The Campbell-Switzer method (CS) is also similarly sensitive [*7*, *24*]. In the present study, we applied GAL and CS to brains diagnosed as corticobasal degeneration (CBD) or progressive supranuclear palsy (PSP), and found a clear-cut discrepancy between GAL and CS. Although little is known about how these argyrophilic properties are engendered [*14*, *18*], "argyrophilia" is now found dependent not only on the sensitivity of each staining procedure but also on the disease process, and, therefore, is of potential importance in differential diagnosis of tauopathies. Moreover, this difference in argyrophilic property may possibly represent different architecture or molecular composition of the deposits.

Materials and methods

Five cases of PSP and three cases of CBD were enrolled in this study. Pathological diagnosis of PSP and that of CBD were based on the published criteria [*11*, *15*]. Additional cases of Down's syndrome (DS) and of AD were used for positive control for GAL and CS. Demographic data on these cases are shown in the Table 1. Coronal slices of cerebral hemispheres were fixed in formalin and embedded in paraffin. Large hemispheric sections were pretreated with potassium permanganate (0.3% for 10 min) followed by oxalic acid (1% for 5 min) [*27*], then stained with the GAL [*4*], and cortical areas rich in GAL-positive structures were sampled for subsequent studies. Neighboring sections from the cortical area rich in GAL-positive structures were stained either with GAL or CS [*7*], and the corresponding argyrophilic structures were compared. Mirror-section pairs (4 μm thick) from these areas were subjected to subsequent studies to identify possible relation between argyrophilia and tau-like immunoreactivity. Pairs of mirror sections were first incubated at 4° C for 2 days with an anti-PHF tau antibody (AT8, 1:10,000, Zwijndrecht, Belgium [*22*]) and the target epitope was visualized with an anti-mouse IgG conjugated with Alexa 488 (1:500, Molecular Probe, Eugene, OR). Sections were then incubated with thiazin red (TR, 1:30,000, Wako, Tokyo, Japan) for 15 min. After being observed under a confocal microscope (Leica TSC/SP, Heidelberg, Germany), one of the section pair was stained with GAL and the other

with CS to compare argyrophilic properties of each AT8- or TR-positive structure. Identification of the same microscopic field on the fluorescence images (AT8 and TR) and on the corresponding silver-stained (GAL and CS) pair-wise images allowed us to compare staining profiles of each structure based on four different properties; AT8 immunoreactivity, affinity to TR, argyrophilia with GAL and that with CS.

Table 1 Demographic data of the cases (*PSP* progressive supranuclear palsy, *CBD* corticobasal degeneration, *DS* Down's syndrome, *AD* Alzheimer's disease)

Pathological diagnosis	Cllinical diagnosis	Age at death (years)	Duration (years)	Gender
PSP	PSP	64	8	F
PSP	PSP	67	8	M
PSP	PSP	68	10	M
PSP	PSP	74	7	F
PSP	PSP	76	10	M
CBD	PSP	49	5	M
CBD	PSP	61	5	M
CBD	CBD	67	7	F
DS	DS	65		M
AD	AD	70		F

Results

On sections from DS/AD brains (Fig. 1), GAL visualized NFTs and neuropil threads (NTs) (Fig. 1A, C). On the neighboring section, CS also visualized NTFs and NTs to an equivalent extent (Fig. 1B, D). In addition, innumerable SPs were visualized with CS, while SPs stained with GAL were limited to those with neuritic reactions. On sections from PSP (Fig. 2A, C) and those from CBD, GAL-positive neurons (Fig. 2A, double arrowhead) and GAL-positive glial structures (Fig. 2A, arrows) were abundant. In contrast, CS, performed on the neighboring section (Fig. 2B,D), failed to visualize any of these GAL-positive structures. Large spherical structures, stained with both GAL (Fig. 2A, arrow) and CS (Fig. 2B, arrow), may be a neuritic plaque probably related to aging process, similar to AD. Plaque-like structure, identified on GAL-stained sections from CBD (Fig. 3A, rectangle; C) and some neurons (Fig. 3A, arrow) were not detectable on the neighboring section stained with CS (Fig. 3B, D).

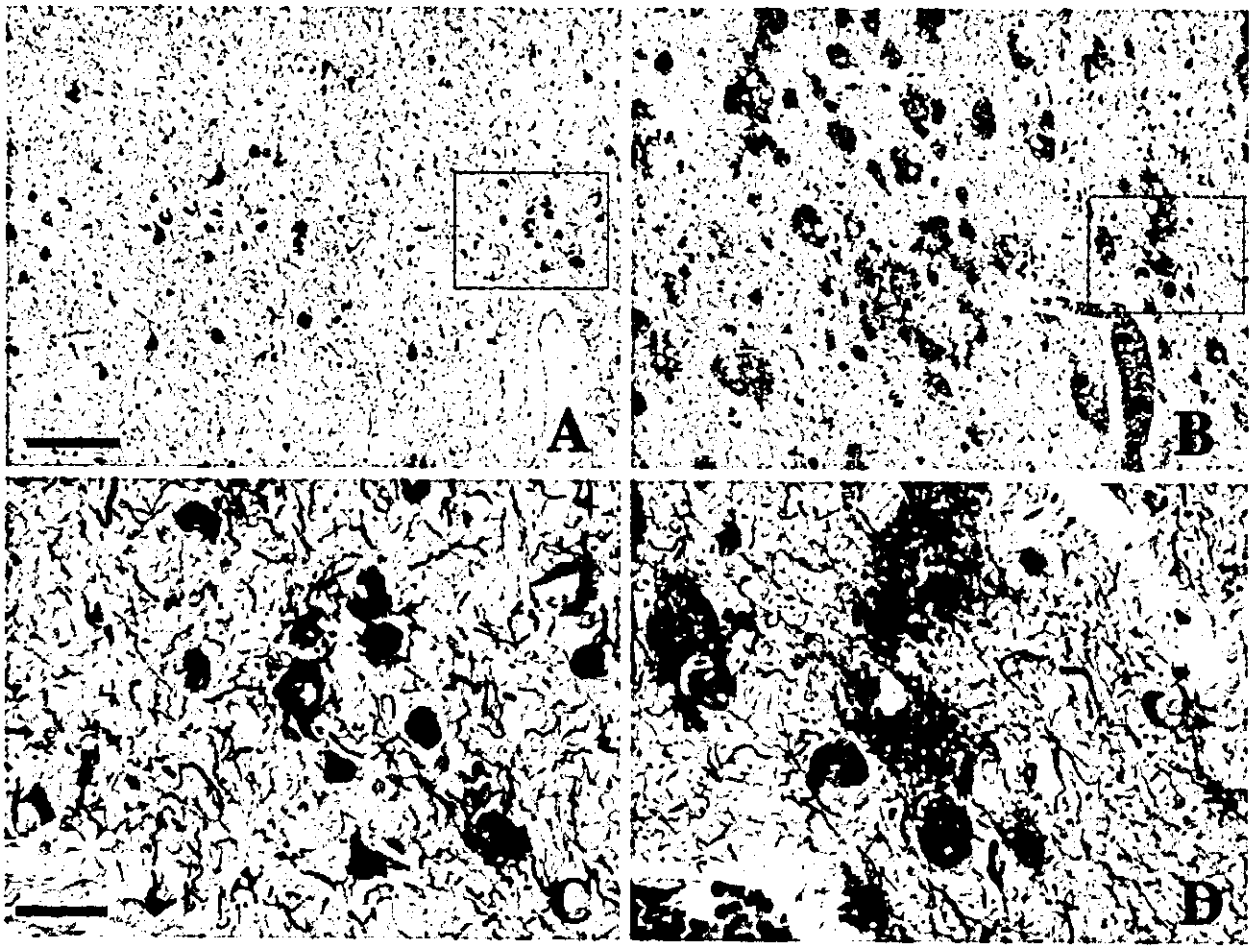

Fig. 1 Temporal cortex from an autopsied patient with DS. NFTs and neuropil threads are widespread to an equivalent extent in both GAL (**A**, **C**: higher magnification of *rectangle* in **A**) and CS-stained sections (**B**, **D**: higher magnification of *rectangle* in **B**). In addition, numerous senile plaques are detectable on CS-stained sections. *Asterisks* indicate the same blood vessels identified on the neighboring sections (*DS* Down's syndrome, *NFTs* neurofibrillary tangles, *GAL* Gallyas staining, *CS* Campbell-Switzer staining). *Bars* **A**, **B**100 μm; **C**, **D** 25 μm

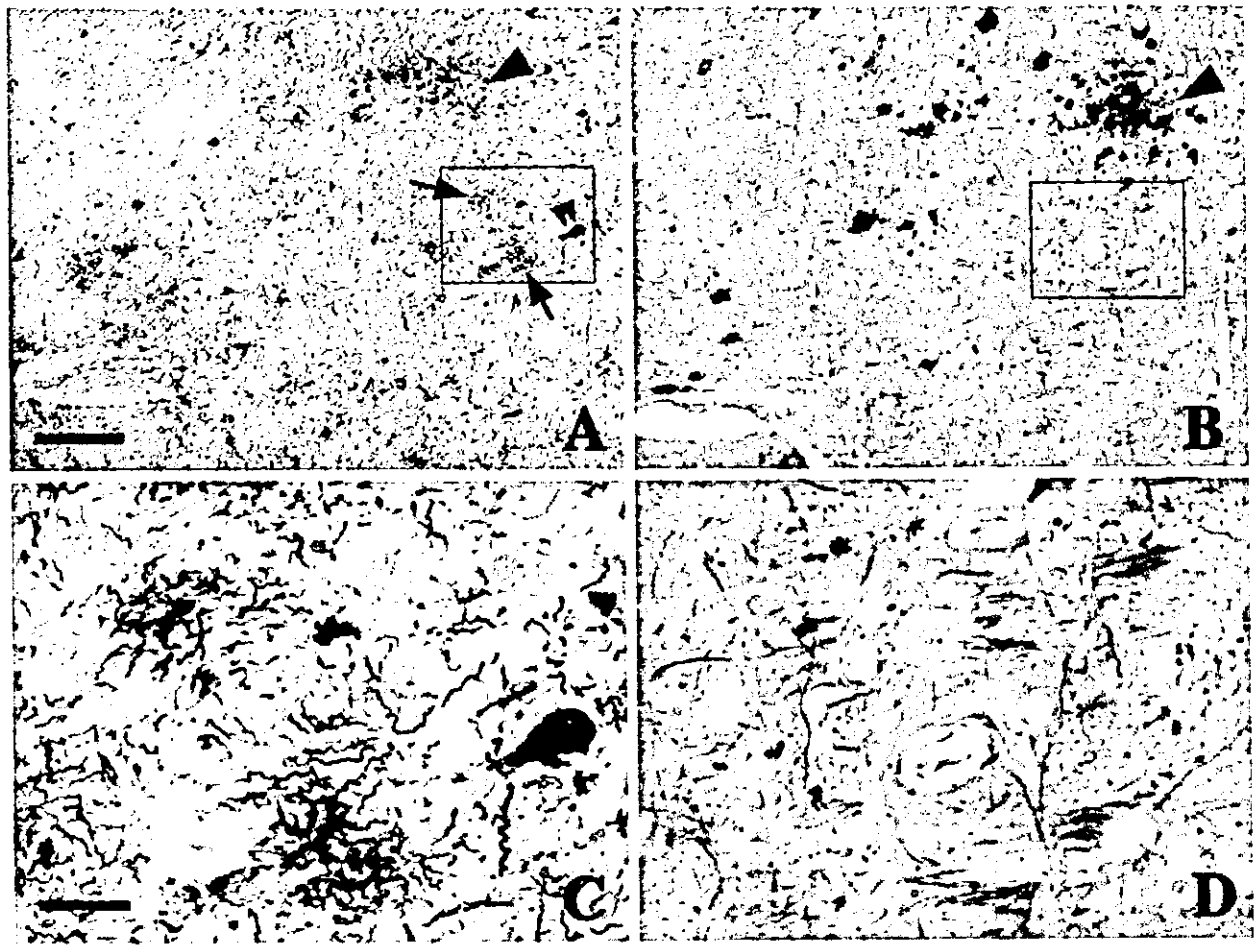

Fig. 2 Neocortex from a patient at autopsy with PSP. In GAL-stained sections (**A**, **C**: higher magnification of *rectangle* in **A**) GAL-positive neuronal (*double arrowhead* in **A**) and glial (*arrows* in **A**) components are numerous. In the same area on the neighboring section stained with CS (**B**), argyrophilic structures are limited to a larger senile plaque (**A**, **B**, *arrowhead*) probably related to aging process. Neither glial nor neuronal deposits, identified on GAL-stained sections, are detected even after CS staining is prolonged to the extent that some normal axons can be detected (**D**). *Asterisks* indicate the same blood vessels identified on neighboring sections (*PSP* progressive supranuclear palsy). *Bars* **A**, **B** 100 μm; **C**, **D** 25 μm

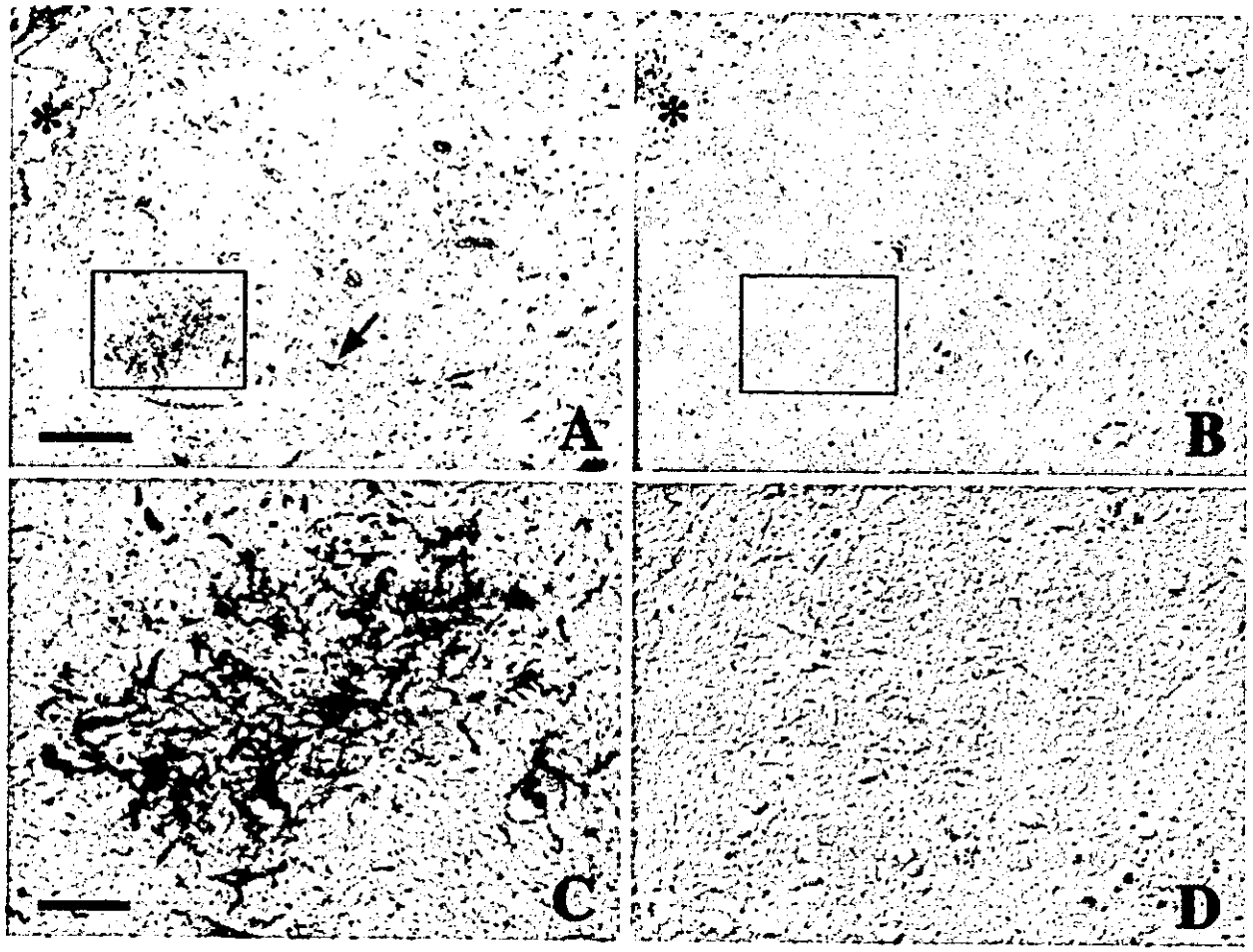

Fig. 3 Neocortex from a patient with CBD. In GAL-stained sections (**A**, **C**: higher magnification of *rectangle* in **A**), astrocytic plaques (*rectangle* in **A**, **C**) and some neurons (*arrow* in **A**) are detectable. Neither of these deposits are detected on the neighboring sections stained with CS (**B**, **D**: higher magnification of *rectangle* in **B**). *Asterisks* indicate the same pial surface on neighboring sections (*CBD* corticobasal degeneration). *Bars* **A**, **B** 100 μm; **C**, **D** 25 μm

This contrast was further confirmed on mirror-section pairs. Fluorolabeling of a mirror-section pair from AD/DS brain with AT8 and TR visualized NFTs and NTs (Fig. 4a–d), that were clearly stained with TR (red, Fig. 4c, d, asterisk) or both TR and AT8 (yellow, Fig. 4c, d, arrowhead), dependent of their evolutionary stage [*29*]. One of the section pair was subsequently stained with GAL (Fig. 4A, C), and the other with CS (Fig. 4B, D). Each of the GAL-positive structures was identifiable on the corresponding mirror section stained with CS, and vice versa. Structures positive for CS and GAL were also positive for TR or for both TR and AT8, (red or yellow, respectively, Fig. 4a–d). Another section pair from PSP brain, initially fluorolabeled (Fig. 4e–h) and subsequently silver-stained either with GAL (Fig. 4E, G) or CS (Fig. 4F, H), demonstrated that each of AT8-positive neurons (Fig. 4g, h, asterisk) was stained with GAL (Fig. 4G, asterisk). CS visualized lipofuscin granules (Fig. 4H, arrowhead) but none of the AT8-positive neurons (Fig. 4H, asterisk). Separation of fluorescence signals (AT8/green and TR/red) demonstrated that affinity to TR was evident (Fig. 4, cTR) in AT8-positive neurons (Fig. 4, cAT8) from DS brain. In contrast, it was absent or at most weak (Fig. 4, hTR) in AT8-positive neurons (Fig. 4, hAT8) from PSP. Astrocytic plaques from a CBD brain were immunoreactive to AT8 (Fig. 4i, j: green, asterisk) and similarly stained with GAL (Fig. 4I, asterisk) but not stained with CS (Fig. 4J,

asterisk).

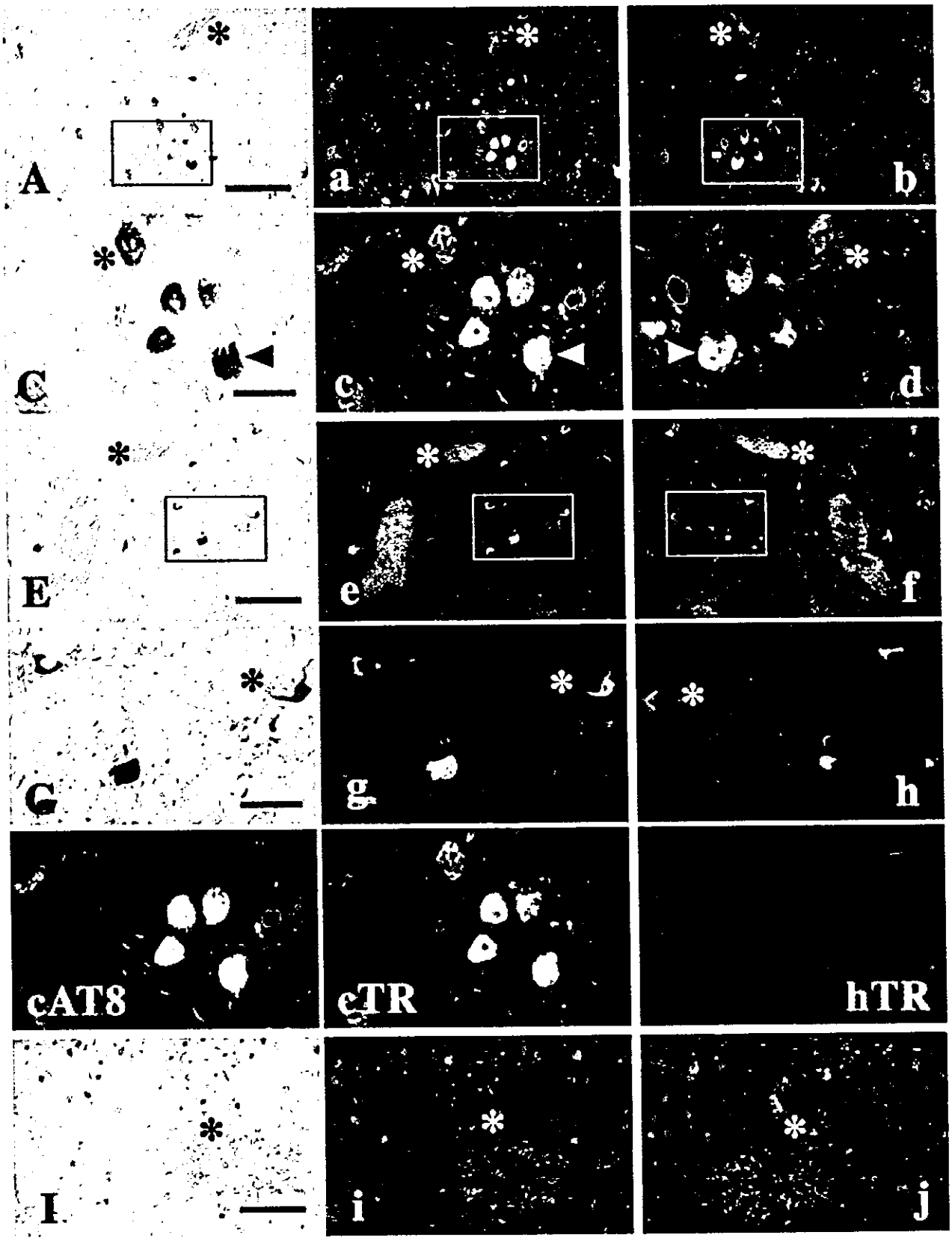

Fig. 4 Mirror-section pairs initially fluorolabeled and subsequently silver-stained. **A**, **a**, **b**, **B** A mirror section pair of the cortex from a DS patient. The same blood vessel is indicated at the top (*asterisk*). **C**, **c**, **d**, **D** Higher magnification of *rectangles* indicated in **A**, **a**, **b** and **B**, respectively. Initially double

stained (**a–d**) with AT8 (*green*) and thiazin red (*TR, red*) and subsequently stained with GAL (**A, C**) or CS (**B, D**). NFTs are stained with TR (*red, asterisk*, **c, d**) or with both TR and AT8 (*yellow, arrowhead*, **c, d**). Each of them are labeled with both GAL (**A, C**) or with CS (**B, D**). **E, e, f, F** A mirror-section pair of the cortex from a PSP patient. The same blood vessel is indicated at the top (*asterisk*). **G, g, h, H** Higher magnification of *rectangles* indicated in **E, e, f, F**, respectively. Each of AT8-positive neurons (*green, asterisk*, **g, h**) is stained with GAL (**G**). CS labeled lipofuscin (*arrowhead*, **H**) but failed to label any of these AT8-positive neurons (**H**, *asterisk*) in PSP. Separation of fluorescence signals from **c** (Down's syndrome) into AT8 (cAT8) and TR (cTR), or those from **h** (PSP) into AT8 (hAT8) and TR (hTR). Affinity of AT8-reactive neurons to TR is evident on the section from Down's syndrome (cTR). It is absent or at most weak on the section from PSP (hTR). **I, i, j , J** A mirror-section pair of the cortex from a CBD patient. A plaque-like structure, positive for AT8 (*green, asterisk*, **i, j**) is stained with GAL (*asterisk*, **I**) but not with CS (*asterisk*, **J**). *Bars* **A, a, B, b, E, e, F, f** 100 μm; **C, c, d, D, G, g, h, H** 30 μm; **I, i, j, J** 50 μm

Discussion

Various methods of silver staining have been introduced to identify pathological structures, related to neurodegenerative processes, and some of them are currently in diagnostic use [*1, 2, 7, 9, 13, 16, 17, 23, 35*]. In spite of their utility, little is known about how the argyrophilic property is engendered [*14, 18, 19, 25*]. Moreover, it is open to question whether argyrophilic properties in different staining methods represent similar processes or features in common, or whether they are different dependent on staining methods [*12, 30, 31*]. In the present study, we have shown that argyrophilic profiles of tau-positive structures differ according to diseases. Each NFT of AD/DS was silver-stained with both GAL and CS. In contrast, tau-positive neocortical neurons and glial components of CBD/PSP were similarly stained with GAL but not with CS. The lack of CS labeling in tau-positive structures in CBD/PSP is in agreement with our previous study that demonstrated a similar paucity of argyrophilia using the Bodian method (BOD) in CBD, while NFTs of AD were, in contrast, stained with BOD [*28*]. Because the number of tau-positive deposits visualized with BOD is smaller than that with GAL [*20*], it is possible that a lower sensitivity of BOD in detecting AD-related deposits is exaggerated in detecting PSP/CBD deposits. CS was initially introduced to label AD-related deposits, especially SPs [*7*]. In this study, comparison of mirror-section pairs stained either with GAL or CS showed that each NFT was equally stained with GAL or CS (Fig. 4), indicating that CS is as sensitive as GAL in detecting NFT. The complete lack of CS labeling in PSP/CBD brains is, therefore, not due to difference in sensitivity between GAL and CS. Procedures for CS and GAL are more easily standardized than other silver-staining methods [*3, 4*]. This excludes the possibility that the complete lack of CS staining in CBD/PSP-related deposits was due to a technical failure. Indeed, all these sections from different diseases were processed simultaneously. Moreover, identification of SPs, probably related to the aging process (Fig. 2), in sections from PSP brains confirmed successful CS staining. CS was therefore found to be useful in distinguishing SPs that may occur on the background of robust tau-related glial pathology in PSP/CBD.

In spite of this sharp contrast either exhibiting (GAL) or not exhibiting (CS) argyrophilia on tau-positive deposits of CBD/PSP, the staining procedure for GAL [*4*] and that for CS [*7*] are quite similar. Alkaline silver iodide is used after pretreatment with lanthanum nitrate for GAL [*4*], while pyridine-silver is the initial step without pretreatment for CS. Because subsequent steps to develop silver particle are essentially identical for GAL and CS, it is likely that the difference in these silver reagents (alkaline silver iodide vs pyridine-silver) is

one of the major factors responsible for this contrast. Its precise mechanism at the molecular level, however, remains to be clarified. One of the current classifications of degenerative tauopathies is based on the biochemical features of tau protein according to three- and four-repeat tau isoforms. It is known that tau-positive deposits of AD/DS are composed of the three- and four-repeat isoforms, while those of CBD/PSP are of predominantly four-repeat isoform [*26*]. Because positive GAL labeling is shared between AD/DS and CBD/PSP, GAL may have an affinity to deposits containing four-repeat tau. Conversely, the lack of CS staining in CBD/PSP is explainable if CS has an affinity to deposits containing three-repeat tau. Indeed, this assumption is compatible because deposits containing both three- and four-repeat isoforms, as in AD/DS, are stained with both CS and GAL. Comparison between AD/DS and CBD/PSP clarified a clear distinction based on silver-staining profile. However, we do not yet know whether this distinction is based directly on difference in tau isoforms or related to more complex composition after tau deposition.

In addition to this complete lack of CS staining, tau-positive deposits in CBD/PSP are characterized by the paucity of TR staining. This possibly represents a relative scarcity of fibrillary composition or different fibrillary composition, as we demonstrated in our previous study [*30*]. The lack of CS staining with abundant GAL staining in cortical neurons of CBD/PSP may be related to this difference. It is then probable that more solid deposition of tau, as seen in AD/DS, is a mixture of three- and four-repeat tau, recognized as NFTs [*29*]. In contrast, deposition of four-repeat tau not accompanied by its three-repeat counterpart is organized into different, probably less fibrillary, structures that escape detection with TR or CS. Our previous study demonstrated that Pick bodies, consisting of predominantly three-repeat isoform of tau, are preferentially stained with BOD but not with GAL [*31*]. This is the reversal of preferential GAL staining seen in CBD/PSP, consisting of predominantly four-repeat isoform of tau. Taken together, each method of silver staining has a preferential affinity to different tau deposits. Although correlation of four-repeat tau deposits to GAL and three-repeat tau deposits to BOD or CS seems consistent, it remains to be determined how each staining method exhibits preferential affinity to corresponding tau deposits in isoform-dependent fashion. Otherwise, this preferential affinity may be dependent on specific deposits, formed in an isoform-dependent manner. Although molecular mechanism to explain how specific argyrophilic properties are engendered still remains to be clarified, these differences will provide with a unique viewpoint to easily recognize specific pathological cascade probably distinct from each other. At present, it is worth being aware of this distinction in search of potential pathological relevance and diagnostic value to be examined in more detail in future studies.

Acknowledgements Supported in part by grants from the Ministry of Health and Welfare, Japan (Longevity Science H-14-005) and the Ministry of Education, Culture, Sports, Science and Technology (grant in aid for scientific research B15300118) to T.U.

References

1. Bodian D (1936) A new method for staining nerve fibers and nerve endings in mounted paraffin sections. Anat Res 65:89

2. Bolle L, Maurer B, Janzer RC (1992) A modified Hortega-Globus stain is superior to Bielschowsky and Bodian stains for demonstrating neuritic plaques. Biotech Histochem 67:82–87 ChemPort PubMed

3. Braak E, Braak H (1999) Silver staining method for demonstrating Lewy bodies in Parkinson's disease and argyrophilic oligodendrocytes in multiple system atrophy. J Neurosci Methods 87:111–115

4. Braak H, Braak E, Ohm TG, Bohl J (1988) Silver impregnation of Alzheimer's neurofibrillary changes counterstained for basophilic material and lipofuscin pigment. Stain Technol 63:197–200
ChemPort PubMed

5. Buée-Scherrer V, Hof PR, Buée L, Leveugle B, Vermersch P, Perl DP, Olanow CW, Delacourte A (1996) Hyperphosphorylated tau proteins differentiate corticobasal degeneration and Pick's disease. Acta Neuropathol 91:351–359
SpringerLink PubMed

6. Bussière T, Hof PR, Mailliot C, Brown CD, Caillet-Boudin M-L, Perl DP, Buée L, Delacourte A (1999) Phosphorylated serine422 on tau proteins is a pathological epitope found in several diseases with neurofibrillary degeneration. Acta Neuropathol 97:221–230
SpringerLink PubMed

7. Campbell SK, Switzer RC, Martin TL (1987) Alzheimer's plaques and tangles: a controlled and enhanced silver staining method. Soc Neurosci Abstr 13:67

8. Connolly AAP, Anderton BA, Esiri MM (1987) A comparative study of a silver stain and monoclonal antibody reactions on Alzheimer's neurofibrillary tangles. J Neurol Neurosurg Psychiatry 50:1221–1224
ChemPort PubMed

9. Cross RB (1982) Demonstration of neurofibrillary tangles in paraffin sections: a quick and simple method using a modification of Palmgren's method. Med Lab Sci 39:67–69
ChemPort PubMed

10. De Silva R, Lashley T, Gibb G, Hanger D, Hope A, Reid A, Bandopadhyay R, Utton M, Strand C, Jowett T, Khan N, Anderton B, Wood N, Holton J, Revesz T, Lee A (2003) Pathological inclusion bodies in tauopathies contain distinct complements of tau with three or four microtubule-binding repeat domains as demonstrated by new sepcific monoclonal antibodies. Neuropathol Appl Neurobiol 29:288–302

11. Dickson DW, Bergeron C, Chin SS, Duyckaerts C, Horoupian D, Ikeda K, Jellinger K, Lantos PL, Lippa CF, Mirra SS, Tabaton M, Vonsattel JP, Wakabayashi K, Litvan I (2002) Office of rare diseases neuropathologic criteria for corticobasal degeneration. J Neuropathol Exp Neurol 61:935–946

12. Duyckaerts C, Brion JP, Hauw JJ, Flament-Durand J (1987) Quantitative assessment of the density of neurofibrillary tangles and senile plaques in senile dementia of the Alzheimer type. Comparison of immunocytochemistry with a specific antibody and Bodian's protocol method. Acta Neuropathol (Berl) 73:167–170

13. Gallyas F (1971) Silver staining of Alzheimer's neurofibrillary changes by means of physical development. Acta Morphol Acad Scient Hung 19:1–8

14. Gambetti P, Autilio-Gambetti L, Papasozomenos SC (1981) Bodian's silver method stains neurofilament polypeptides. Science 213:1521–1522

ChemPort PubMed

15. Hauw JJ, Daniel SE, Dickson D, Horoupian DS, Jellinger K, Lantos PL, McKee A, Tabaton M, Litvan I (1994) Preliminary NINDS neuropathologic criteria for Steele-Richardson-Olszewski syndrome (progressive supranuclear palsy). Neurology 44:2015–2019
ChemPort PubMed

16. Hicks SP (1946) A rapid pyridine silver stain for nervous tissue and reticular fibers. J Lab Clin Med 31:1375–1377

17. Hirano A, Zimmerman HM (1962) Silver impregnation of nerve cells and fibers in celloidin sections. A simple impregnation technique. Arch Neurol 6:114–122
ChemPort PubMed

18. Iqbal K, Braak E, Braak H, Zaidi T, Grundke-Iqbal I (1991) A silver impregnation method for labeling both Alzheimer paired helical filaments and their polypeptides separated by sodium dodecyl sulfate-polyacrylamide gel electrophoresis. Neurobiol Aging 12:357–361
crossref ChemPort PubMed

19. Kondoh H, Matsushita M, Kosaka K, Miyazaki N (1993) Staining senile plaques using Bodian's method modified with methenamine. Biotech Histochem 68:113–116
ChemPort PubMed

20. Lamy C, Duyckaerts C, Delaère P, Payan C, Fermanian J, Poulain V, Hauw JJ (1989) Comparison of seven staining methods for senile plaques and neurofibrillary tangles in a prospective series of 15 elderly patients. Neuropathol Appl Neurobiol 15:563–578

21. Mailliot C, Sergeant N, Bussière T, Caillet-Boudin M-L, Delacourte A, Buée L (1998) Phosphorylation of specific sets of tau isoforms reflects different neurofibrillary degeneration processes. FEBS Lett 433:201–204
crossref ChemPort PubMed

22. Mercken M, Vandermeern M, Lübke U, Six J, Boons J, Van de Voorde A, Martin J-J, Gheuens J (1992) Monoclonal antibodies with selective specificity for Alzheimer Tau are directed against phosphatase-sensitive epitopes. Acta Neuropathol 84:265–272
ChemPort PubMed

23. Reusche E (1991) Silver staining of senile plaques and neurofibrillary tangles in paraffin sections. A simple and effective method. Pathol Res Pract 187:1045–1049
ChemPort PubMed

24. Rosenwald A, Reusche E, Ogomori K, Teichert H-M (1993) Comparison of silver staining and immunohistology for the detection of neurofibrillary tangles and extracellular cerebral amyloid in paraffin sections. Acta Neuropathol 86:182–186
SpringerLink PubMed

25. Switzer RC III (1993) Silver staining methods: their role in detecting neurotoxicity. Ann NY Acad Sci 679:341–348
PubMed

26. Tolnay M, Probst A (1999) Tau protein pathology in Alzheimer's disease and related disorders. Neuropathol Appl Neurobiol 25:171–187

crossref ChemPort PubMed

27. Uchihara T, Kondo H, Ikeda K, Kosaka K (1995) Alzheimer-type pathology in melanin-bleached sections of substantia nigra. J Neurol 252:485–489

28. Uchihara T, Mizusawa H, Tsuchiya K, Kondo H, Oda T, Ikeda K (1998) Discrepancy between tau immunoreactivity and argyrophilia by the Bodian method in neocortical neurons of corticobasal degeneration. Acta Neuropathol 96:553–557
[SpringerLink] ChemPort PubMed

29. Uchihara T, Nakamura A, Yamazaki M, Mori O (2001) Evolution from pretangle neurons to neurofibrillary tangles monitored by thiazin red combined with Gallyas method and double immunofluorescence. Acta Neuropathol 101:535–539
ChemPort PubMed

30. Uchihara T, Nakamura A, Yamazaki M, Mori O, Ikeda K, Tsuchiya K (2001) Different conformation of neuronal tau deposits distinguished by double immunofluorescence with AT8 and thiazin red combined with Gallyas method. Acta Neuropathol 102:462–466
ChemPort PubMed

31. Uchihara T, Ikeda K, Tsuchiya K (2003) Pick body disease and Pick syndrome. Neuropathology 23:318–326
crossref PubMed

32. Vallet PG, Guntern R, Hof PR, Golaz J, Delacourte A, Robakis NK, Bouras C (1992) A comparative study of histological and immunohistochemical methods for neurofibrillary tangles and senile plaques in Alzheimer's disease. Acta Neuropathol 83:170–178
[SpringerLink] ChemPort PubMed

33. Wilcock GK, Matthews SM, Moss T (1990) Comparison of three silver stains for demonstrating neurofibrillary tangles and neuritic plaques in brain tissue stored for long periods. Acta Neuropathol 79:566–568
[SpringerLink] ChemPort PubMed

34. Wisniewski HM, Wen GY, Kim KS (1989) Comparison of four staining methods on the detection of neuritic plaques. Acta Neuropathol 78:22–27
ChemPort PubMed

35. Yamaguchi H, Haga C, Hirai S, Nakazato Y, Kosaka K (1990) Distinctive, rapid, and easy labeling of diffuse plaques in the Alzheimer brain by a new methenamine silver stain. Acta Neuropathol 79:569–572
[SpringerLink] ChemPort PubMed

36. Yamamoto T, Hirano A (1986) A comparative study of modified Bielshowsky, Bodian and Thioflavin S stains on Alzheimer's neurofibrillary tangles. Neuropathol Appl Neurobiol 12:3–9
ChemPort PubMed

37. Yen SH, Horoupian DS, Terry RD (1983) Immunocytochemical comparison of neurofibrillary tangles in senile dementia of Alzheimer type, progressive supranuclear palsy, and postencephalitic parkinsonism. Ann Neurol 13:172–175
ChemPort PubMed